SANDIA REPORT

SAND2000-8727
Unlimited Release
Printed August 2001

Corrosion of Alloys and Metals by Molten Nitrates

R. W. Bradshaw, S. H. Goods

Prepared by
Sandia National Laboratories
Albuquerque, New Mexico 87185 and Livermore, California 94550

Sandia is a multiprogram Laboratory operated by Sandia Corporation, a Lockheed Martin Company, for the United States Department of Energy under Contract DE-AC04-94AL85000.

Issued by Sandia National Laboratories, operated for the United States Department of Energy by Sandia Corporation.

Available to DOE and DOE contractors from
U.S. Department of Energy
Office of Scientific and Technical Information
P.O. Box 62
Oak Ridge, TN 37831

Telephone:(865)576-8401
Facsimile:(865)576-5728
E-Mail: reports@adonis.osti.gov
Online ordering: http://www.doe.gov/bridge

Available to the public from
U.S. Department of Commerce
National Technical Information Service
5285 Port Royal Rd
Springfield, VA 22161

Telephone:(800)553-6847
Facsimile:(703)605-6900
E-Mail: orders@ntis.fedworld.gov
Online order: http://www.ntis.gov/ordering.htm

SAND 2000-8727
Unlimited Release
Printed August 2001

CORROSION OF ALLOYS AND METALS BY MOLTEN NITRATES

R. W. Bradshaw
Materials Chemistry Department

S. H. Goods
Materials Mechanics Department
Sandia National Laboratories/CA

ABSTRACT

This review paper examines the corrosion behavior of alloys and metals in molten salts consisting of alkali metal nitrates. The chemistry of this class of molten salt is discussed as it affects the composition of the melt and metal oxide solubility. The corrosion rates and mechanisms of a broad selection of alloys are reviewed, including stainless steel, carbon steel, chromium-molybdenum steel, nickel and nickel alloys. The type of corrosion products that are formed on these materials over a wide range of experimental conditions are discussed. The results of studies of the effect of the molten salt on mechanical properties and cracking behavior of a number of alloys are also summarized.

ACKNOWLEDGMENTS

Sandia National Laboratories is a multiprogram laboratory operated by Sandia Corporation, a Lockheed Martin company, for the United States Department of Energy under contract DE-AC04-94AL85000.

Table of Contents

Page

This page intentionally left blank

Corrosion of Alloys and Metals by Molten Nitrates

I. Introduction

Molten nitrate salts are used primarily as heat transfer fluids in the chemical and metallurgical industries [1], although other technological applications are being developed. The prospective applications include solar thermal energy (STE) systems [2] and separation of oxygen from air.[3] Other potential uses have been suggested, including batteries [4], fuel cells [5], and flue gas scrubbers for air pollution control.[6] STE systems have been the most intensive new development. A 10 megawatt solar thermal electric power system that uses focussed sunlight has recently been demonstrated [7] and construction of a commercial-scale power plant is planned.[8] Solar thermal energy systems that use molten alkali nitrate salts as working fluids for heat collection and storage require structural materials that have good corrosion resistance at temperatures up to 600°C. Selecting container materials for such advanced applications raises several questions regarding adequate corrosion resistance for long-term service.

The corrosion behavior of alloys and metals in molten salts consisting of alkali nitrates or nitrate/nitrite mixtures is reviewed in this paper with primary emphasis placed on the suitability of materials for engineering applications. The database regarding corrosion behavior in these molten salts has expanded substantially since the comprehensive review by Rahmel in 1982 [9], particularly with regard to the variety of materials investigated as well as to corrosion at temperatures above 500°C. Such progress was primarily a result of the development of solar thermal energy applications that employ this molten salt to collect and store the energy of focussed sunlight. In this review, the corrosion behavior of classes of alloys suitable for fabricating STE components are summarized and the temperature envelopes for using these materials are estimated. The corrosion rate equations and mechanisms are discussed with regard to the equilibrium chemistry of the molten salts.

II. Chemistry of Molten Alkali Nitrates

Molten nitrate salts are used industrially almost exclusively as mixtures of $NaNO_3$ and KNO_3. The liquid-solid boundary in the phase diagram for these two constituents does not indicate a sharp eutectic, but rather, a broad range of low-melting mixtures surrounding the minimum melting point of 222°C at the equimolar ratio (46 wt.% $NaNO_3$).[10] The composition 44 mol.% $NaNO_3$ - 56 mol.% KNO_3 (60-40 wt.%), which melts at 238°C, was chosen for advanced STE applications and was used in several engineering demonstration projects.[7,11] The data suggested that a mixture enriched in $NaNO_3$ relative to KNO_3 would be desirable since the significantly lower cost of the sodium salt would offset the disadvantages of a slightly increased melting point. Low cost is particularly important if the molten salt is to serve as the thermal energy storage media given the large inventories required.[7]

A principal consideration in accepting the "60-40" molten salt composition for long-term use at temperatures near 600°C was chemical stability because the evolution of decomposition products can affect both its thermophysical properties and corrosion potential. Molten nitrate salts may undergo a variety of reactions depending on the temperature and the composition of the cover gas.[12] The primary reaction with regard to long-term stability is the decomposition of nitrate to nitrite and oxygen; see Eq. 1.

$$NO_3^- \Leftrightarrow NO_2^- + 1/2\ O_2 \qquad \text{Eq. 1}$$

Experimental investigations of the equilibrium of Eq. 1 have determined the equilibrium constant at temperatures up to 600°C.[13] The nitrite concentration of melts in equilibrium with air is about 3 wt.% at 565°C and 5.5 wt.% at 600°C. Decomposition (formation of nitrite) is suppressed by increasing the pressure of oxygen in the cover gas. Fig. 1 compares the concentration of nitrite according to whether the 60-40 nitrate mixture was equilibrated with air or oxygen. Calculated values (lines) and measured values (circles) of the nitrite concentration at various temperatures are shown and agree well.[36]

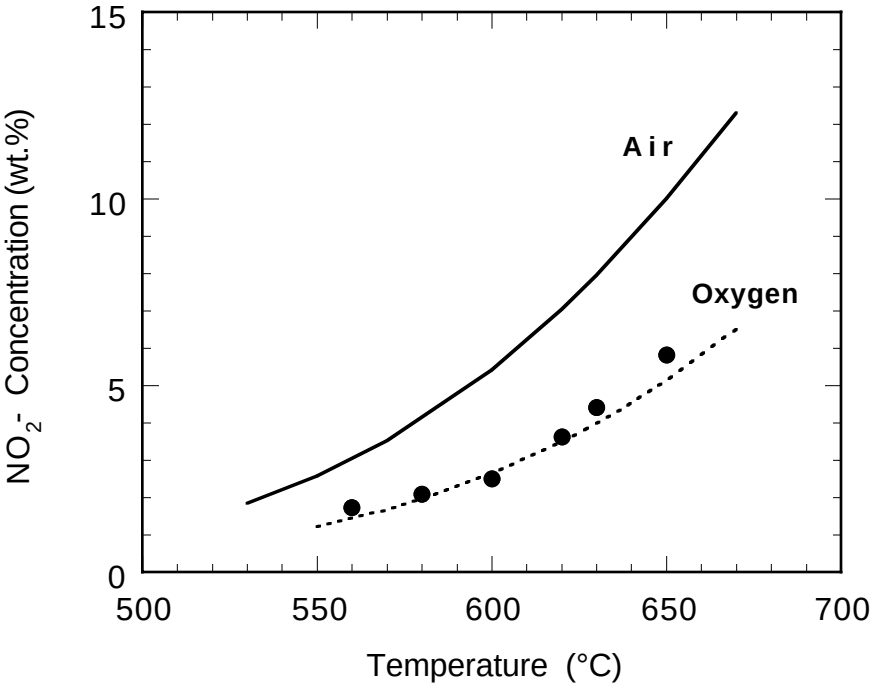

Figure 1. Equilibrium concentration of nitrite in molten nitrate salt vs. temperature. The cover gas is either air or oxygen. The lines represent calculated values and the symbols denote experimental measurements.

Another important chemical property of molten nitrates, with regard to corrosion, is that these melts behave as bases in the Lux-Flood sense, that is, as oxide ion donors. Molten nitrates are quite weak bases, at least at temperatures below 600°C.[14] Thermochemical equilibrium calculations have been used to predict the behavior of nitrate melts over a wide range of conditions. The thermodynamic model included reactions of nitrate and nitrite which yield alkali oxides and gases, such as oxygen, nitrogen and NOx and estimated the phase stability diagram of the Na-O-N system at various temperatures.[15] This study determined that the concentration of oxide ions was negligible at STE design temperatures, but increased rapidly above 600°C. This was an important finding because oxide ions are known to exacerbate corrosion. A comparison of the oxide ion concentrations measured in equilibrium melts with predictions of the thermodynamic calculations suggested that oxide ions behave non-ideally in nitrate melts.[16]

Some of the chemical and electrochemical factors relevant to corrosion of metals in molten nitrates have been discussed by Smryl.[17] Of particular interest is that chromium (as well as molybdenum and manganese) can produce soluble anions, e.g., chromate or dichromate. Because of this solubility, chromium can be readily extracted from the surface oxide scales formed on many types of alloys designed for high temperature applications. The chemical behavior of molybdenum in molten nitrate salts is similar to that of chromium and as such, it is likely that molybdenum is also removed from the surface oxide layers. Molybdenum forms

oxides (MoO_2, MoO_3) that can react with trace amounts of oxide ions in the weakly basic molten salt to form molybdate, MoO_4.[14] In contrast, nickel and iron do not form soluble species.[17]

Compilations of the physical properties of molten nitrates are available.[18] However, the maximum operating temperature intended for STE systems is 600°C, which is significantly higher than the limits of the published properties. For this reason, a research program was undertaken to measure the physical properties of the equimolar mixture of $NaNO_3$ and KNO_3 over the complete range of temperatures relevant to advanced STE systems. The results of this experimental program, encompassing viscosity, heat capacity, density, and thermal conductivity, have been summarized elsewhere.[19]

III. Corrosion of Fe-Cr-Ni Alloys

The corrosion behavior of iron-chromium-nickel alloys in molten alkali nitrates is of primary importance for applications that require prolonged containment of the melt at temperatures nearing 600°C, and STE systems in particular. These alloys, which include the austenitic 300-series stainless steels particularly, are essential for fabricating components subjected to both large mechanical stresses and elevated temperature. Corrosion data from a variety of sources prior to 1970 have been compiled by Bohlmann,[20] however, these data concern short-term tests and were not considered adequate for engineering design. Furthermore, little information was available regarding the types of corrosion products formed or the kinetics of the corrosion process. During the preceding 20 years, a good deal of data have been collected from either the immersion of test coupons in isothermal salt baths or the exposure of alloy tubing in thermal convection flow loops or pumped loops. Below, we review key results from a variety of these studies. In subsequent sections, results pertaining to a variety of other alloys and metals are discussed.

Laboratory studies performed at Sandia National Laboratories by Bradshaw, Goods, and others have shown that Fe-Cr-Ni alloys corrode at quite moderate rates at temperatures up to 600°C in a molten salt consisting of 60% (wt.) $NaNO_3$ and 40% KNO_3. Isothermal crucible experiments were conducted at 570°C and the extent of corrosion was measured from descaled weight losses. The total metal losses of 316SS and 304SS were about 10 microns after 7,000 hours of exposure.[21,22] Experiments conducted at 560°C produced similar results.[23] Corrosion experiments were also performed using low-velocity fluid flow loops in which coupons were exposed to the molten salt at 600°C. Under these conditions, Alloy 800 (Incoloy® 800, nominally Fe-20Cr-35Ni; Incoloy® 800 is a registered tradename of Inco Alloys International, Huntington, WV, USA.) experienced about 6 microns of metal loss after 5000 hours [24], while 304SS lost about 8 microns after 4200 hours.[25] Corrosion data obtained from a molten salt pipe loop pumped at a relatively large flow rate agreed with these results and further demonstrated the adequate corrosion resistance of 316SS and 304SS.[26]

The kinetics of metal loss and scale formation of stainless steels in molten nitrates generally follow a parabolic rate equation at temperatures approaching 600°C.[23] Such an equation describes corrosion that increases proportionally with the square root of time and indicates the formation of a protective, or self-limiting, corrosion product layer on the surface of an alloy. This behavior is indicated in Fig. 2 with regard to the corrosion of 304SS at 570°C in several commercial-purity mixtures of molten nitrates. In Fig. 2, descaled metal losses are plotted vs. the square root of time. Plotted in this way, the good fit of the data to straight lines affirms the applicability of a parabolic rate equation. The parabolic rate constants are approximately 1×10^{-7} $cm/sec^{1/2}$. Thus, the corrosion rate of stainless steel in molten nitrates is less than in a high-pressure steam environment at the same temperature.[27]

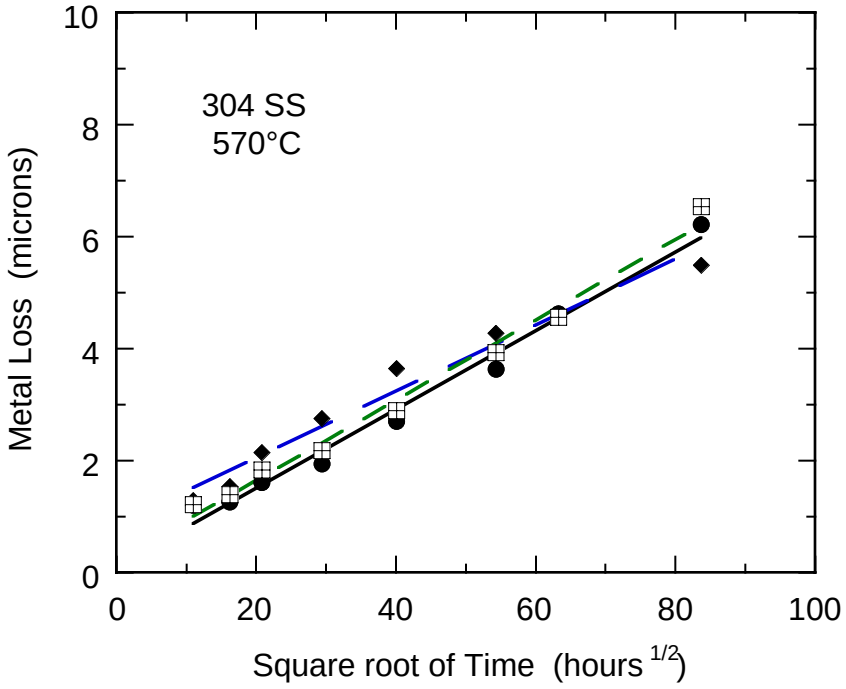

Figure 2. Descaled metal losses of Type 304 SS during corrosion in molten nitrate salt at 570°C. Data for several commercial-purity nitrate mixtures are shown.

Examination of the corrosion scale layers on stainless steel coupons following the tests described above revealed that adherent oxide layers were formed that had a multilayer structure. This morphology was found to be characteristic of oxides formed on all Fe-Cr-Ni alloys at temperatures up to 600°C. This morphology is shown in the SEM micrograph in Fig. 3 in which three distinguishable layers of oxide are indicated. The elemental composition of these layers, and the underlying alloy, is given by the electron microprobe analysis shown in Table 1. The "spot #" in Table 1 corresponds to the locations labeled on Fig. 3. The oxide layers (dark band at top) consists primarily of the iron oxide magnetite, Fe_3O_4, as identified by X-ray diffraction.[21,23] The exterior portion of the oxide was partially converted to a sodium-iron oxide, while the innermost layer is a spinel of iron and chromium that provides the protective layer with regard to the corrosion rate. These results have been corroborated by analyses of alloy tubes from experimental solar receivers. Examination of scale layers on the inside surface of Alloy 800 receiver tubes, that had operated for about 1000 hours in a cyclic solar radiation environment, revealed similar oxide layers.[28] These studies established that the primary corrosion products were M_3O_4 spinels of iron alone and iron mixed with chromium and that chromium was depleted from the alloys and dissolved in the melt.

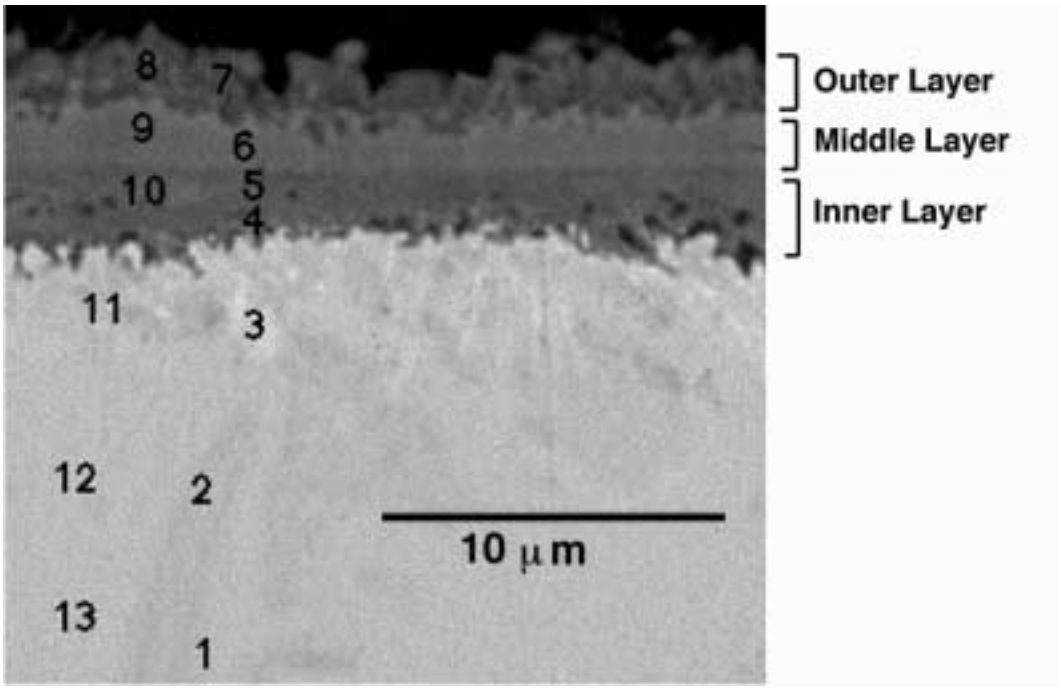

Figure 3. Photomicrograph of the corrosion product layers on 316 SS after 4084 hours of thermal cycling at 560°C (max.) in molten nitrate salt.

TABLE 1. Elemental concentration (wt.%) of selected areas of the corrosion product layers on 316 SS after 4084 hours of thermal cycling at 560°C in molten nitrate salt.

Region	Spot #	O	Fe	Cr	Ni	Mo	Na
Outer layer	7,8	13.3	69.4	1.4	1.9	0	12.3
Middle layer	6.9	12.0	76.9	3.3	1.2	0.9	4.5
Inner layer	4	18.1	13.2	63.2	1.3	3.0	0.7
"	5	16.8	21.4	54.7	4.8	1.2	0
"	10	16.1	27.0	46.2	7.5	2.4	0
Depletion band	3	0	71.9	6.3	18.5	2.6	0
"	11	0	72.7	7.7	9.1	3.9	0
Alloy	1,13	0	68.4	18.9	9.0	3.4	0
"	2,12	0	66.4	18.9	11.9	2.8	0

Corrosion of stainless steels in molten nitrate salts is also influenced by factors such as thermal cycling and the presence of dissolved impurities in the molten salt. Due to the diurnal cycling of solar insolation, the high-temperature components in an STE system are required to tolerate many temperature excursions between the maximum operating temperature and the minimum ambient temperature. Thermal cycling generally aggravates high temperature oxidation, but the degree to which a particular material is affected in any given environment is difficult to predict. The primary effect of thermal cycling on high-temperature oxidation is to damage protective surface oxide layers via mechanical stresses arising from mismatched thermal expansion coefficients between the surface scale and the alloy. Corrosion is also affected by the presence of dissolved chloride impurities in the molten salt.

Typically, the least costly grades of nitrate salts tend to have higher impurity concentrations, thus, it was necessary to assess the impact of such constituents on corrosion. A previous corrosion study of both stainless and carbon steels showed a moderate effect of dissolved chlorides on corrosion.[21] Thermal cycling and impurities in the molten salt act in concert to increase corrosion rates, in that chloride often degrades adhesion of thermally-grown oxides to high temperature alloys.[29]

The effect of both of these factors on the metal losses of 316SS thermally-cycled between 565°C and about 100°C is shown in Fig. 4. This plot uses parabolic coordinates, thus the upward deviation of the metal losses for coupons exposed to molten salts containing more than 0.5 wt.% chloride (M-3 and M-4) demonstrates that the protective surface oxide, formed at low chloride concentrations, has been degraded. In this case, a linear rate equation has replaced the parabolic one. Although the linear rate constants pertaining to this test are not remarkably large, metal recession will obviously be much greater during prolonged service than when protective scales form.

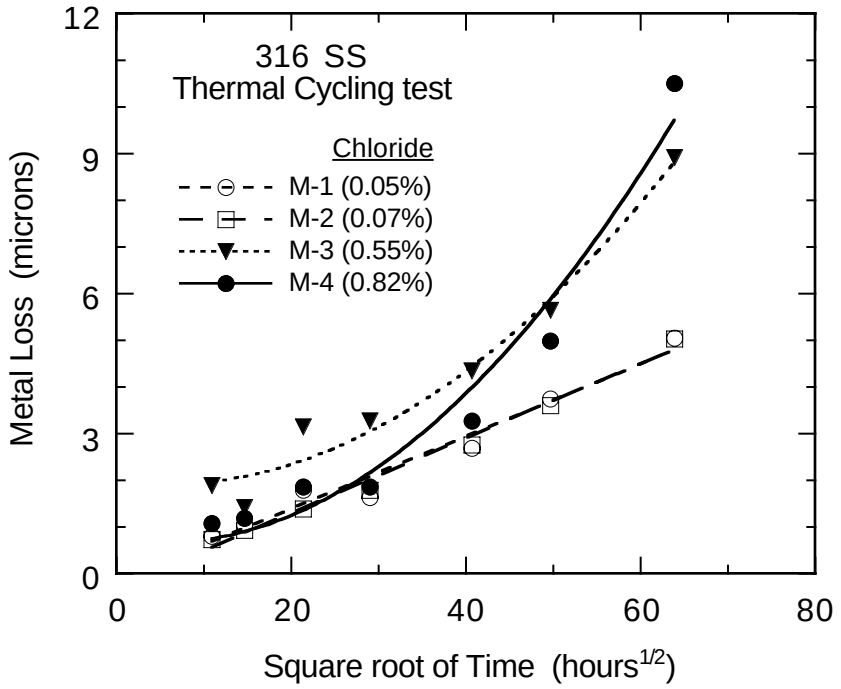

Figure 4. Descaled metal losses of Type 316 SS during thermal cycling corrosion in molten nitrate salt mixtures at 565°C (max.). Data for four different levels of dissolved chloride are shown.

Corrosion in Thermal Convection Flow Loops

Corrosion of Fe-Cr-Ni alloys has also been studied using thermal convection flow loops. Thermal convection loops create a circulatory fluid flow due to buoyancy differences resulting from an imposed temperature differential.[30] Such an apparatus can be used to study mass transport of dissolved alloying elements, caused by fluid flow along the thermal gradient, as well as corrosion. The concern with regard to solubility behavior was that dissolved corrosion products might precipitate in the coldest parts of the flow system and foul or plug them, a phenomena called thermal-gradient mass transfer. The alloys 316SS, 304SS, and Alloy 800 were investigated by Bradshaw using loops that operated at temperatures between 300°C and 600°C. The rates of metal losses of these alloys were between 5 and12 micron/year at 600°C.[24,25] A similar study by Tortorelli and DeVan, using thermal convection loops in which the salt was in contact with an argon cover gas instead of the air atmosphere used in the former experiments, estimated corrosion rates of about 8 microns/year for both 304SS and 316SS at 590°C.[31] These values agree well with expectations based on the data discussed above obtained from isothermal tests at somewhat lower temperatures. Measurements of metal losses by chemical descaling revealed that the majority of metal consumption was due to oxide scale

formation rather than depletion of alloying elements as soluble species.[24] However, chemical analyses of the salt in the loops established that chromium was gradually dissolved, whereas iron and nickel were negligibly soluble. As discussed in a preceding section, the solubility of chromium in molten nitrates is quite large. However, the dissolution of chromium into the melt was kinetically limited by diffusion through the surface oxide scale. Thus, the concentration of chromate in the molten salt is limited to amounts far below solubility limits. Accordingly, no thermal-gradient mass transfer was observed.

Corrosion at Temperatures Exceeding 600°C

The corrosion resistance of Fe-Cr-Ni alloys deteriorates significantly at temperatures exceeding 600°C. As noted in the preceding section concerning molten salt chemistry, decomposition of the nitrate melt ultimately forms oxide ions and these species are much more corrosive than nitrate. Slusser, et al, evaluated a large number of alloys in molten nitrates at temperatures up to 670°C and reported metal losses of as much as 120 microns in tests lasting several hundred hours.[32] Other studies found that significant changes in the primary corrosion products occur in this temperature regime. The major change is that the spinel oxides described above are converted to sodium ferrite ($NaFeO_2$).[33] This compound has been observed at temperatures of 615°C and higher. This change in corrosion mechanism also results in rapid corrosion rates that follow linear kinetics, indicating that $NaFeO_2$ is a non-protective scale.[34,35] Corrosion tests have recently been conducted in a molten nitrate salt mixture that was stabilized by using an oxygen cover gas to suppress decomposition of the molten salt. Coupons were exposed to this salt at temperatures up to 650°C and corrosion rates were determined by descaled weight losses. Metal losses were approximately ten times greater at 650°C than at 570°C and the iron-chromium spinel observed at the lower temperature had been completely converted to the sodium-containing oxide by the basicity of the molten salt.[36]

IV. Corrosion of Cr-Mo Steels

Chromium-molybdenum steels are often used for the evaporator sections of steam generators operating at temperatures up to 500°C rather than stainless steels in order to avoid stress corrosion cracking. In applications involving molten nitrates, these alloys must, of course, also exhibit satisfactory corrosion resistance. Only limited data have been available concerning the corrosion behavior of Cr-Mo steels in molten nitrate salts until recently. Bohlmann compiled corrosion data prior to 1972 based upon a survey of industrial users of molten nitrates and estimated that $2^1/_4$Cr-1Mo and 5Cr-$^1/_2$Mo would corrode about 200 microns/year at 480°C.[20] Spiteri reported that $2^1/_4$Cr-1Mo experienced linear metal loss kinetics equal to about 800 microns/year at 500°C when the alloy was exposed to nitrate salt under a nitrogen cover gas.[37] Corrosion data have also been reported for molten salts containing high proportions of nitrites, such as 40 (wt.%) $NaNO_2$-7 $NaNO_3$-53 KNO_3. Kirst, Nagle and Castner observed corrosion rates as large as 250 microns/year for low chromium steels immersed for several weeks at 538°C.[38] At 500°C, Fe-5Cr steel corroded according to linear kinetics at a rate of nearly 300 microns/year.[39] Kramer, Smyrl and Estill did not report rate data, but identified Fe_2O_3 as the primary corrosion product on 5Cr-$^1/_2$Mo at 450°C.[40]

Laboratory studies by Bradshaw have provided a better understanding of the oxidation behavior of chromium-molybdenum steels in molten nitrates and have established reliable limits on the use of these materials. Several Cr-Mo steels containing from $2^1/_4$ to 9 wt.% chromium were studied in a molten nitrate salt at 460°C.[41] The descaled weight losses observed in these tests are plotted vs. the square root of time in Fig. 5. The $2^1/_4$ Cr-1Mo steel lost about 50 mg/cm^2, equivalent to about 60 microns of metal recession, during the 4000 hour test period. Although

parabolic rate equations generally described the corrosion of all three steels, significant differences were apparent. The corrosion resistance increased as the chromium content of the steels increased, but 9Cr-1Mo corroded much slower than the steels containing either $2^1/_4$Cr or 5Cr. Note that the weight loss of 9Cr-1Mo was multiplied by a factor of ten (10) to provide resolution in Fig. 5. The experimental data presented above show that $2^1/_4$ Cr-1Mo steel corroded quite rapidly in molten alkali nitrate salt at 460°C. In addition, the chloride impurities typically contained in commercial grades of alkali nitrates significantly aggravated corrosion of this alloy.

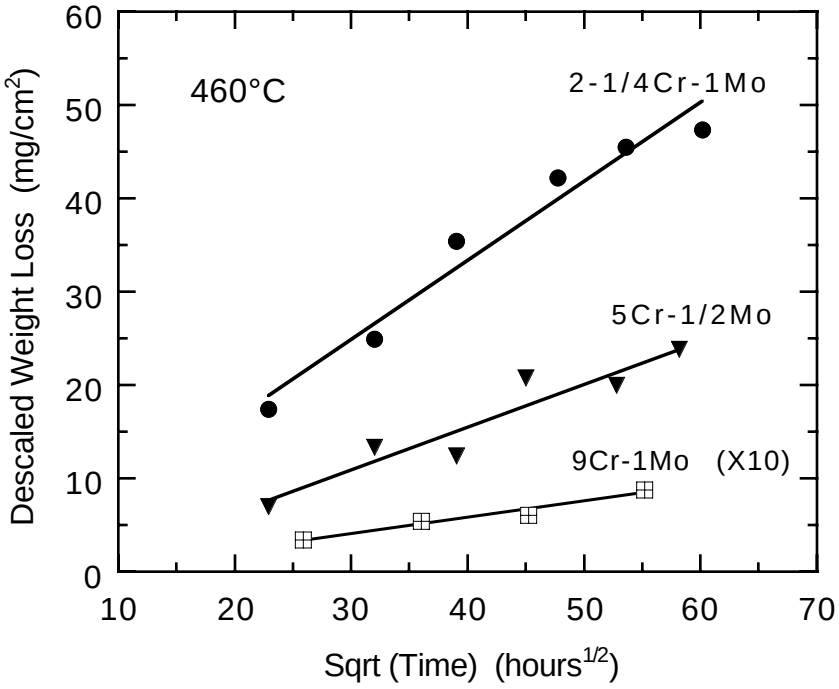

Figure 5. Effect of the chromium content of Cr-Mo steels on metal losses in molten nitrate salt at 460°C.

Metallographic examination of the corrosion products revealed that complex oxide phases were formed during corrosion in the molten salt on the steels containing less than 9% Cr. As an example, Fig. 6(a) shows a scanning electron micrograph of the residual oxidation products formed on a $2^1/_4$ Cr-1Mo steel after 4200 hours of exposure to the molten salt. The oxide layer was composed of many discrete lamellae that were organized on several dimensional scales. Near the salt-exposed surface, these lamellae are only about 1 micron in thickness. Near the alloy interface, the fine lamellae are less evident, but are still visible at very high magnification. On a coarser scale, bands of many of these lamellae, approximately 10-20 microns thick, are delineated by porosity or cracks. Fig. 6(b) is an X-ray map of chromium taken from the same location that reveals that each band appears to be partitioned into alternating layers, approximately 5-10 microns thick, consisting of Cr-rich and Cr-poor iron oxide. In contrast, the 9Cr-1Mo steel formed a single bilayer oxide consisting of Fe_3O_4 over a layer of $(Fe,Cr)_3O_4$,where both layers were basically the same thickness, about 2 microns.[41]

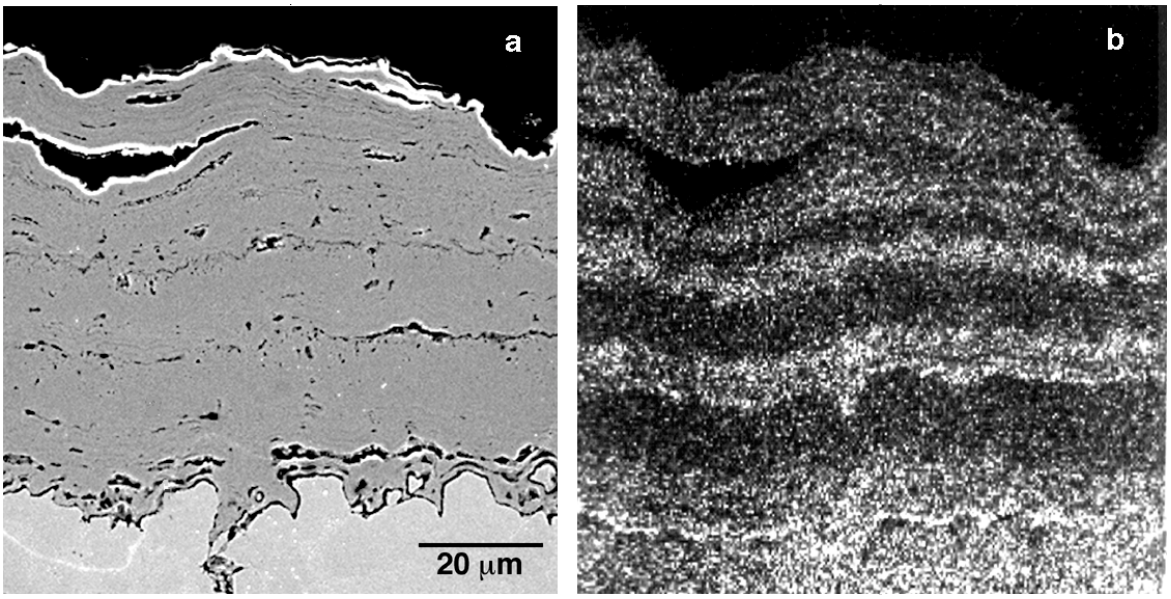

Figure 6. (a) Scanning electron micrograph showing the morphology of the oxide scale formed on $2^1/_4$Cr-1Mo after 4200 hours of exposure to molten nitrates at 460°C. Discrete lamellae of oxide that are organized on several dimensional scales are apparent. (b) X-ray map of chromium, corresponding to micrograph, reveals that each oxide band is partitioned into alternating layers, approximately 5-10 μm thick, that consist of Cr-rich (bright) and Cr-poor iron oxide.

The use of Cr-Mo steels for molten nitrate salt containment in STE systems is currently restricted to alloys containing 9 wt.% chromium or more, which affords suitable corrosion resistance. A leaner alloy, such as $2^1/_4$Cr-1Mo, can only be considered if the corrosion resistance can be significantly improved. There is evidence in the literature that relatively small additions of silicon improve the corrosion resistance of Fe-Cr alloys in gaseous oxidants at high temperature. For example, Taylor, et al., observed that 0.6 wt.% silicon significantly decreased the parabolic rate constant of an Fe-9Cr alloy, compared to the pure binary alloy, oxidized in CO_2 at 580°C.[42] Laboratory experiments were conducted by Bradshaw and Goods to evaluate the effect of small additions of silicon to $2^1/_4$Cr-1Mo on corrosion resistance in molten nitrates.[43] Corrosion measurements based on descaled weight losses showed that steels containing 1 wt.% and 2 wt. % silicon, respectively, experienced two to ten times less corrosion than the standard alloy that contains 0.36 wt.% Si during a 4200 hour testing interval. These data are plotted in

Fig. 7. These tests further demonstrated that the silicon-enriched steels had a substantial tolerance to chloride contamination of the molten salt. In addition, the corrosion products formed on the silicon-enriched alloys were considerably more adherent and much less likely to blister than the standard alloy.

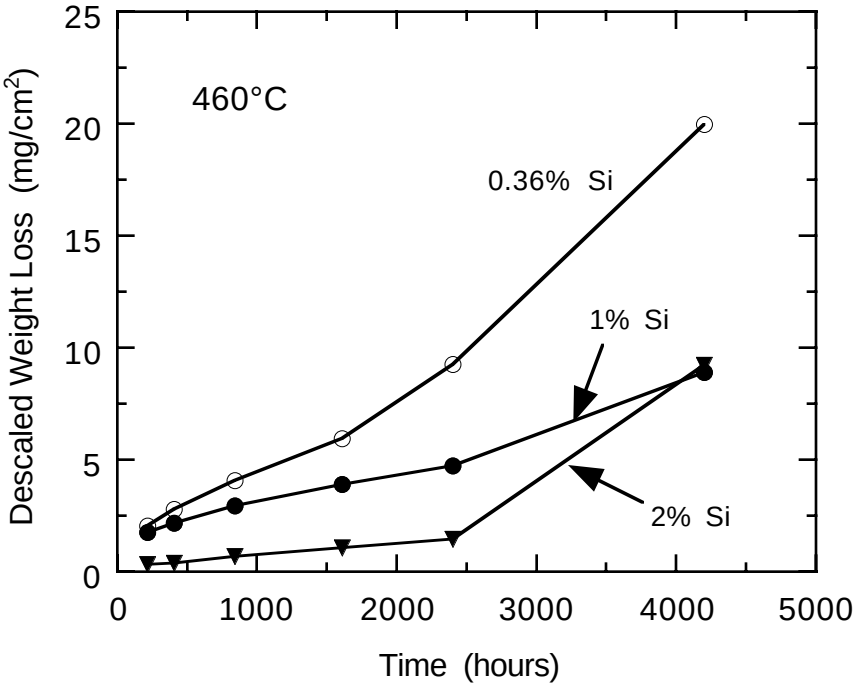

Figure 7. Effect of the silicon content of 2-1/4 Cr-1 Mo steel on metal losses in molten nitrate salt at 460°C.

V. Corrosion of Carbon Steel

In applications where exposure to nitrate salts can be limited to 400°C or less, the use of carbon steels may be considered. Several papers in the literature describe the results of short-term corrosion tests of carbon steel in molten nitrates. These investigations primarily concerned the effect of dissolved impurities, such as chloride and sulfate, on corrosion as compared to pure nitrate melts. For example, El Hosary, et al, reported that the corrosion rate of mild steel at 400˚C increased approximately as the logarithm of the chloride concentration.[44] At 0.6 wt.% NaCl, the corrosion rate increased by a factor of about three compared to a chloride-free melt during an 8-hour test. Other researchers report similar behavior for iron at 400°C-450°C.[45] Corrosion rates increased by about a factor of four during a 25-hour test when the chloride concentration was 0.7 wt.% compared to a chloride-free melt. The effect of dissolved sulfate in nitrate melts on corrosion of mild steel results in corrosion rates increased by 20% when 7.5 wt.% Na_2SO_4 was added to the pure molten salt.[46]

Long-term experiments have been conducted to verify the corrosion resistance of carbon steel in commercial-purity nitrate salts. Measurements of net weight gains suggested that corrosion rates of carbon steel are suitable for components of STE systems that operate at temperatures below about 320°C.[26] Experiments have also been performed in which corrosion was measured directly, as the descaled weight loss, for pure $NaNO_3$-KNO_3 salt, the same salt containing 0.7 wt.% chloride, and a ternary salt mixture containing $Ca(NO_3)_2$ as well as the alkali nitrates. Weight loss data for A36 carbon steel specimens at 316°C are shown in Fig. 8.[21] The data fall into two distinct categories depending on the impurities present in the molten salt. The specimens exposed to the high-purity molten salt and the chloride-doped mixtures (upper 3 lines) corroded slowly at this temperature and lost about 1 to 3 mg/cm^2 after 4000 hours. Weight losses increased as the chloride level increased. The specimens exposed to the ternary nitrate salt (lower solid line) corroded very slowly, losing only 0.3 mg/cm^2 after 4000 hours. A binary salt mixture that contained several hundred ppm (wt.) of dissolved magnesium (dotted line) corroded at an intermediate rate.

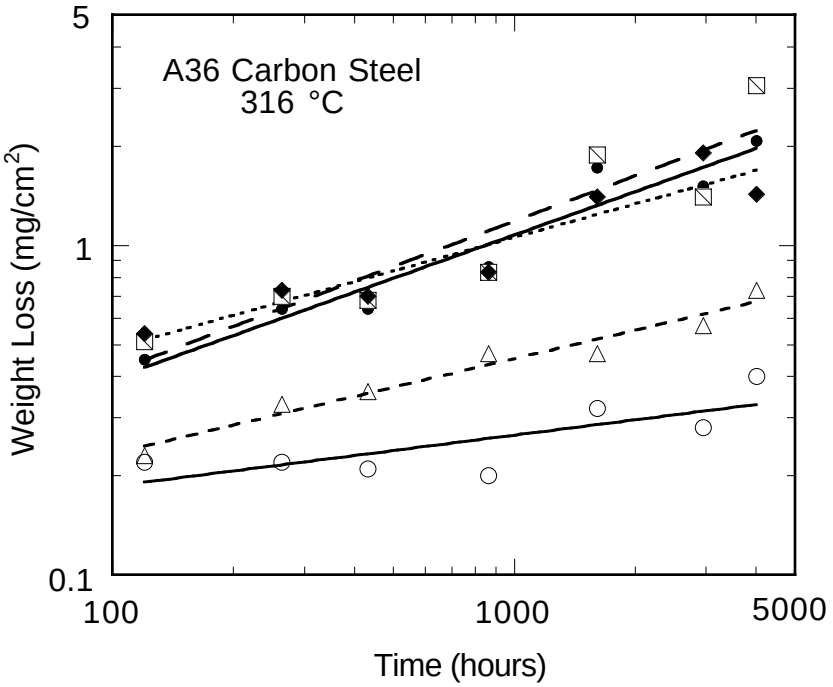

Figure 8. Descaled metal losses of A36 carbon steel during corrosion in molten nitrate salt mixtures at 316°C. Data for several concentrations of dissolved chloride are shown. The open symbols denote experiments in which the molten salt contained several hundred ppm (wt.) of magnesium.

The oxidation products that formed on carbon steel after prolonged exposure to the molten salt have been analyzed by X-ray diffraction and determined to be primarily magnetite.[21] The oxide films formed on A36 carbon steel that displayed unusually small weight losses, in the ternary molten salt described above, have been examined by Auger spectroscopy coupled with sputter depth profiling. This analysis demonstrated that magnesium replaced iron on a majority of the divalent sites in the spinel lattice, and thereby created a significantly more protective oxide film than magnetite.[47]

VI. Corrosion of Nickel and Nickel-Base Alloys

Nickel-base alloys are also candidates for molten nitrate salt applications and generally possess superior mechanical strength compared to the iron-base alloys. The low solubility of nickel

oxide, observed during the experiments with stainless steels discussed above, suggests that nickel may form a protective oxide layer in the molten salt. Some information has been published concerning corrosion of nickel and its alloys in molten $NaNO_3$-KNO_3 at temperatures relevant to advanced solar thermal energy systems. Corrosion tests conducted in molten $NaNO_3$ at temperatures between 465°C and 529°C for 6944 hours resulted in losses of about 30 microns/year for a group of nickel-base alloys that included IN-600 (Inconel® 600, nominal composition, Ni-15Cr-9Fe; Inconel® 600 is a registered tradename of Inco Alloys International, Huntington, WV, USA.), Ni-20Cr and Ni-16Cr-22Fe.[48] In a nitrite-rich molten salt consisting of 52 (wt.%) KNO_3-41 $NaNO_2$-7 $NaNO_3$, a corrosion rate of 450 microns/year was observed at 570°C for Inconel® 600 and corrosion kinetics were linear.[20] Burolla and Bartel reported metallographic analysis of corrosion products on Inconel® 600 following an immersion of 700 hours in $NaNO_3$-KNO_3 at 550°C that revealed internal oxidation of chromium and formation of nickel-rich and iron-rich surface oxide scales.[49] Slusser, et al, observed rapid corrosion of a variety of nickel-base alloys in molten nitrates at temperatures exceeding 650°C.[32]

More recent laboratory studies have provided a somewhat better understanding of the oxidation behavior of nickel and its alloys in molten nitrates.[50] The corrosion of commercial purity nickel, (Nickel 200 grade), a nickel- 4% aluminum alloy (Ni-4Al), and IN-600 was studied at various temperatures in the eutectic nitrate melt. The corrosion products formed on nickel and its alloys were very adherent, thus net weight gain, due to oxide formation, provided a convenient measurement of the extent of corrosion. The net weight gains of these materials are shown in Fig. 9. In general, the trends of weight gain with time indicate that corrosion proceeded according to linear rate equations. Note that the corrosion experiments with the alloys were performed at 600°C and 630°C, compared to 565°C for nickel metal.

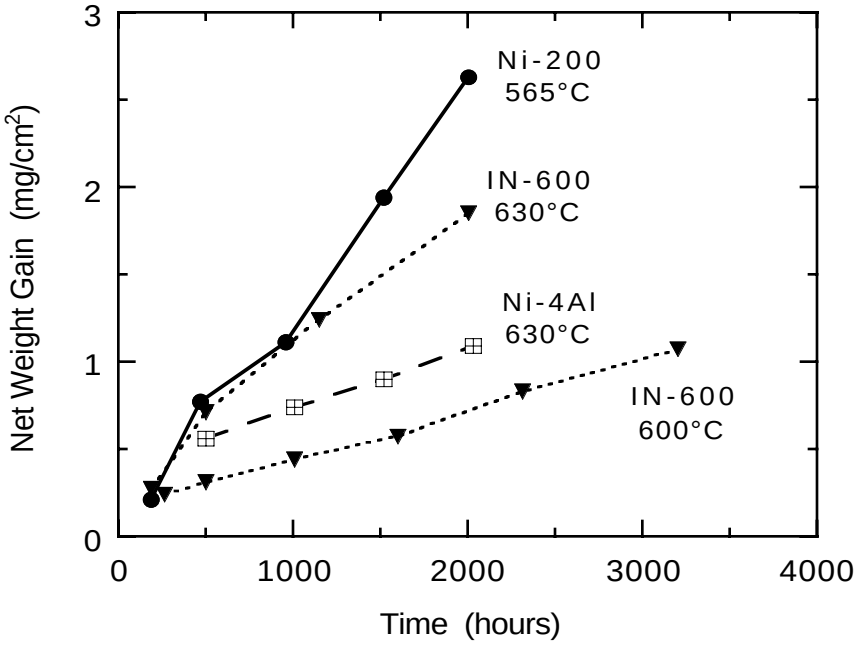

Figure 9. Net weight changes of Nickel 200, IN-600, and Ni-4 Al immersed in molten nitrate salt at various temperatures.

Metallographic examination of cross-sections of the test coupons revealed quite different corrosion products between nickel and the two alloys. The optical micrograph in Fig. 10 shows that Ni-200 suffered severe intergranular oxidation at 565°C. After 1500 hours, thick layers of nickel oxide formed along the grain boundaries and these intrusions had penetrated well over 100 microns into the metal. This behavior was apparently due to the relatively large carbon content of Ni-200 (0.08 wt.%). Bricknell has described similar oxidation morphology of Ni-200 in gaseous oxidants and attributed the attack to carbon at grain boundaries.[51]

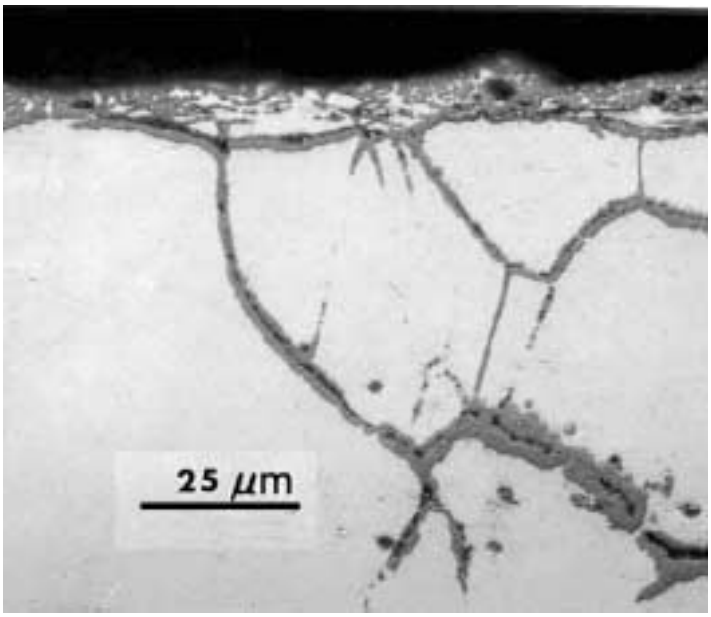

Figure 10. Micrograph showing intergranular oxidation of Nickel 200 after exposure to molten nitrate salt at 565°C for 1500 hours.

Metallographic examination of IN-600 after 2800 hours at 630°C revealed a different mechanism of oxidation than for nickel. The micrograph in Fig. 11 shows that the oxidation products consisted of an external layer of NiO (the narrow dark band above the light band) about 4 microns thick. Chromium was absent from the NiO layer that contacts the molten salt. However, internal oxidation of chromium had penetrated to a depth of almost 40 microns. The bright band beneath the oxide layer is metallic nickel and contains no alloying elements. Soluble corrosion products of chromium were also formed.

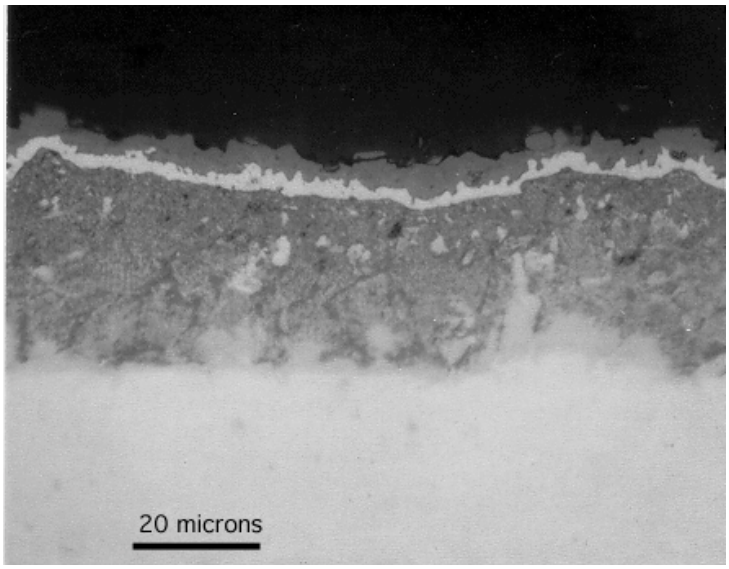

Figure 11. Micrograph showing surface scale and internal oxidation of Inconel 600 after exposure to molten nitrate salt at 630°C for 2800 hours.

VII. Molten Salt Effects on Mechanical Properties

The material performance requirements, other than general corrosion resistance, for molten salt containment alloys have been driven largely by STE applications. In this regard, requirements vary considerably between STE subsystems. For "cold salt" storage tanks, carbon steels have been shown to have adequate corrosion resistance up to 320°C and the mechanical requirements are minimal, resulting only from the thermal cycling-induced stresses and strains along the tank sidewall as the salt level rises and falls. The most challenging salt containment requirements were found in the receiver tubing where the combination of the one-sided heating and the diurnal nature of receiver operation give rise to severe thermomechanical stresses. These operating conditions are manifested as a low-cycle, high-strain amplitude fatigue environment. A key concern that arose because of the unique operating characteristics of the receiver was whether the exposure to the molten salt, in conjunction with the thermomechanical environment, would promote corrosion-induced cracking of the tubing material. Conversely, the question arose as to whether prolonged exposure to nitrate salts would degrade the mechanical properties of various alloys in some fashion that would adversely affect their fatigue properties. The complexity of testing in molten salts limited studies to a few alloys such as Alloy 800, 316 SS and HT-9, a 12Cr-1Mo ferritic steel The influence of molten salts on mechanical properties of $2^1/_4$Cr-1Mo steel has been examined as well. Because of the difficulty in reproducing the precise thermomechanical environment experienced by the receiver tubes, most tests have been of a screening nature, usually consisting of monotonic tensile tests performed at very low strain rates.

Constant Extension Rate Testing (CERT) of Alloys

The CERT test (also called the slow strain rate test) consists of imposing a constant displacement rate on a tensile specimen of uniform gauge section that is exposed to the environment of interest. Multiple tests are usually performed over a wide range of strain rates to allow for prolonged exposure times. It is not unusual, therefore, for individual tests to run for up to 1000 hours. Because of the somewhat arbitrary test conditions, the results are usually compared to tests performed on specimens exposed to a reference environment under identical conditions of strain rate and temperature. Typically, reduction in area (RA), strain to fracture and ultimate tensile strength (UTS) are measured as parameters that determine the susceptibility of an alloy to environmental degradation. The test is thus a versatile method for the detection of an

environmental or stress corrosion cracking phenomenon. It may also be used for the analysis of the critical variables which may contribute to the observed material degradation. The variables which may be screened include temperature, the nitrate salt composition or impurity content, and the metallurgical condition of the alloy. The CERT test may also be used to examine the influence of deformation on the corrosion characteristics of a material subjected to an oxidizing environment. In particular, for solar thermal applications, it is important to determine if mechanical deformation induces either a change in corrosion mode (from one of uniform surface attack to one that is intergranular in nature) or if it appreciably accelerates the rate of oxidation, resulting in an unacceptable metal loss rate.

Early work examined the CERT response of Alloy 800, 316 SS and HT-9 at 600°C and $2^1/_4$Cr-1Mo at both 450°C and 525°C in nitrate salts.[52,53] The behavior of sheet tensile specimens in molten salt was compared to the behavior of specimens exposed to air over the same range of strain rate. Fig. 12 shows the influence of a 60 wt.% $NaNO_3$ – 40 wt.% KNO_3 molten salt mixture on the ductility of these alloys. Ductility loss in the figure is simply computed as the difference in ductility measured in air minus the ductility measured in the salt mixture. For 316 SS, little or no ductility loss due to the salt is apparent over the entire range of strain rates examined. However, both the ferritic steel and Alloy 800 begins to show some small decrease in ductility at the lowest strain rates corresponding to salt exposure times of approximately 1000 hours. In contrast, the lower alloy steel demonstrated marked decrease in ductility even at the substantially lower test temperatures.

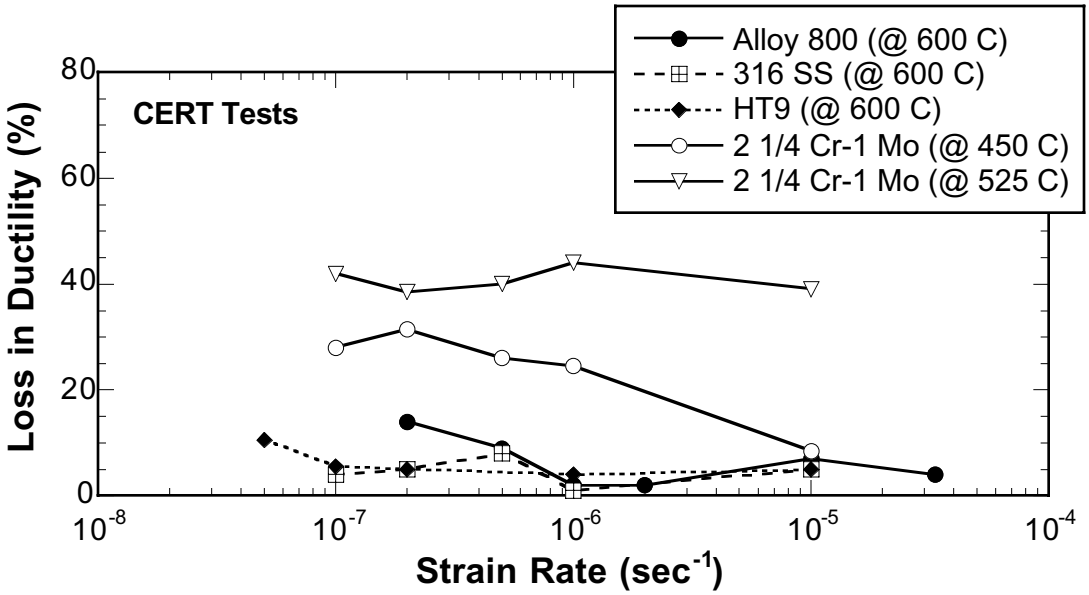

Figure 12. The influence of molten salt exposure on the ductility of high temperature alloys.

Metallographic analysis revealed that the continuously imposed deformation resulted in two principal effects for Alloy 800 and 316 SS. First, there is some intrusion of the oxide film below the nominal oxide-base metal interface. An example of this is shown in Fig. 13(a) for Alloy 800 tested at a strain rate of 2×10^{-7} sec^{-1}. This intrusion occurred due to a small amount of near-surface, grain boundary cracking induced by the slow strain rates and elevated temperature. Away from the immediate vicinity of the fracture surface, this cracking extended to a depth of only one or two grain diameters. Further, such cracking was ubiquitous, occurring at these temperatures and strain rates regardless of the environment. Cracking was therefore not an indication of a transition from a relatively benign mode of uniform surface corrosion to an aggressive form of intergranular attack.

Continuous straining of these alloys in concert with exposure to the molten salt, however, also resulted in some acceleration of the rate of oxidation. The effect was small, constituting only about a twofold increase in the rate of oxide film formation. In contrast, Fig. 13(b) shows that continuous deformation resulted in a catastrophic acceleration in surface corrosion rates for the $2^1/_4$Cr-1Mo alloy, leading to the observed loss of ductility.

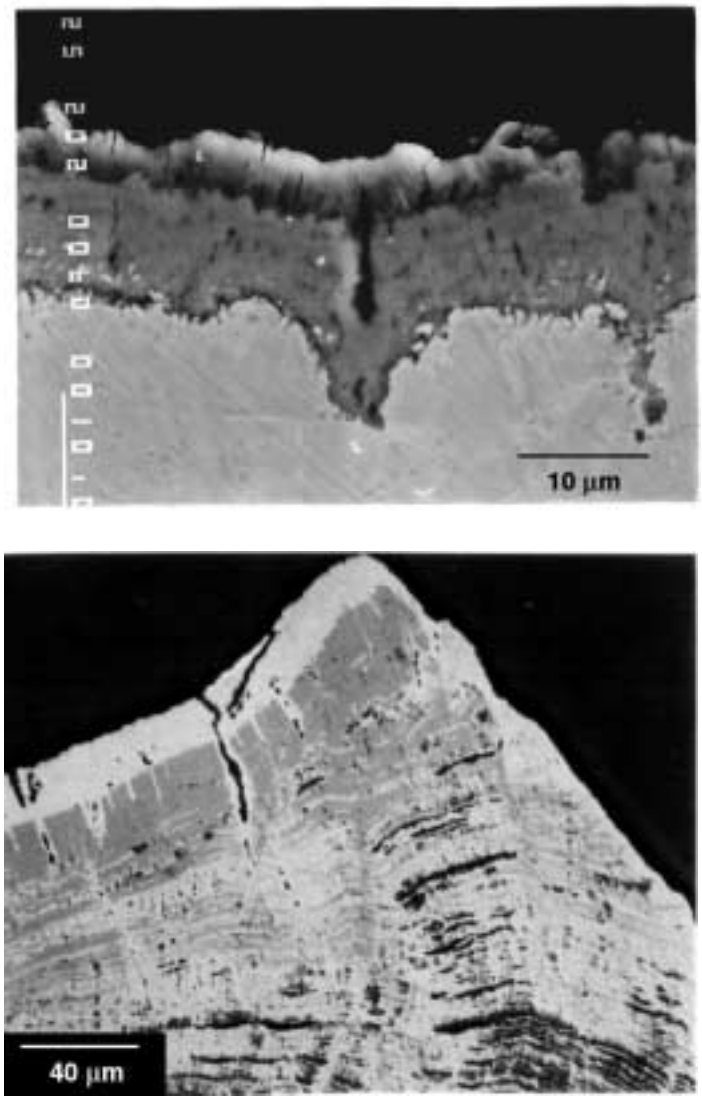

Figure 13. Surface oxide films formed on Alloy 800 (upper) and $2^1/_4$Cr-1Mo (lower) specimens subjected to continuous deformation.

Corrosion-Fatigue Behavior

A very limited number of studies have examined the behavior of alloys in fatigue environments. In one study, hollow tubes of Alloy 800 (at two carbon levels) were filled with the 60 wt.% $NaNO_3$ – 40wt.% KNO_3 salt mixture and then tested under low-cycle, high strain amplitude fatigue conditions.[54] The results of these tests are shown in Fig. 14 and reveal that salt exposure had little effect on the fatigue life of the alloy, compared to specimens exposed to air. These tests were performed isothermally at 650°C and thus did not fully replicate the

thermomechanical environment of the receiver. More importantly, total exposure times to the molten salt were quite short. At the lowest strain amplitude, the maximum test time was about 40 hours, while at the highest strain amplitudes, test times were only a few hours. These exposure times contrast with a receiver lifetime requirement of nominally 30 years. Given the relatively slow oxidation rates of this alloy reported above, such short tests produced little interaction between the molten salt and the test material.

The fatigue crack growth characteristics of Alloy 800 in molten nitrate salt have also been examined.[55] Pre-cracked specimens were immersed in the same nitrate salt mixture as above and tested at 600°C. While suffering from the same shortcomings as the above work, namely isothermal exposure conditions and limited salt exposure times, the results revealed that the salt-induced formation of oxidation products had little effect on fatigue crack growth rates or crack growth thresholds.

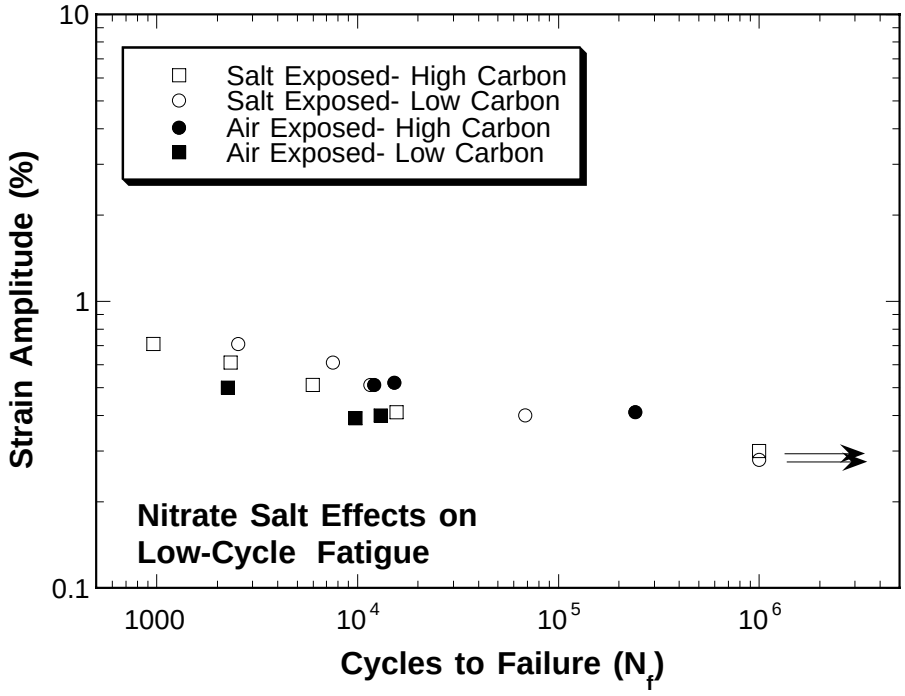

Figure 14. Corrosion-fatigue behavior of Alloy 800 in molten nitrate salt at 650°C.

VIII. Summary

A comprehensive database regarding the corrosion resistance of a variety of alloys and metals in molten nitrate salts has been established that enables materials to be selected with confidence in their long-term performance. Fe-Cr-Ni alloys, e.g., austenitic stainless steels, display acceptable corrosion resistance up to 600°C, regardless of whether thermal cycling is imposed or moderate amounts of chloride impurities are dissolved in the molten salt. Protective surface scales, consisting of spinel oxides of iron and iron-chromium, are formed on these alloys and parabolic corrosion kinetics were observed. Chromium was oxidized and slowly dissolved from Cr-containing alloys by the molten salt, although thermal gradient mass transfer was not observed. Corrosion rates of iron-base alloys increased rapidly at temperatures exceeding 600°C due to fluxing of chromium from the oxide scale and formation of sodium iron oxide. Cr-Mo steels offer corrosion resistance if the chromium content is at least 9% or supplemental silicon is added to $2^1/_4$Cr -1Mo steel. Carbon steels are corroded very slowly at temperatures up to at least 320°C. Nickel experienced rapid intergranular oxidation at 565°C, although nickel-chromium alloys demonstrated good oxidation resistance. The molten salt did not cause susceptibility to cracking of high-temperature alloys or appear to reduce the corrosion-fatigue lifetime.

IX. References

1. B. W. Hatt and D. H. Kerridge, Chem. Britain, 15 (2), (1979), p. 78.

2. P. DeLaQuil, B. Kelly and R. Lessley, Solar Energy Mater., 24 (1991), p. 151.

3. B. R. Dunbobbin and W. R. Brown, "Pilot Plant Development of a Chemical Air Separation Process", Air Products and Chemicals, Inc., Allentown, PA, DOE/CE/40544-1, Feb. 1987.

4. N. Q. Minh and L. Redey, in Molten Salt Techniques, Vol. 3, D. G. Lovering and R. J. Gale, Editors, Plenum Press, (1987), p. 228.

5. F. Palmisano, L. Sabbatini and P. G. Zambonin, J. Chem. Soc. Faraday Trans. I, 80 (1984), p. 1029.

6. S. I. Cheng, H. Pitlick and R. Siegel, Environ. Sci. Tech., 5 (1971), p.79.

7. M. R. Prairie, J. E. Pacheco. G. J. Kolb and J. P. Sutherland, "Solar Central Receiver Technology: The Solar Two Project", 1996 Annual A.I.Ch.E. Heat Transfer Conference, Houston, TX, Aug. 3-5, 1996.

8. J. E. Pacheco. G. J. Kolb and C. E. Tyner, "Summary of the Solar Two Test and Evaluation Program", Renewable Energy for the New Millennium, Sydney, Australia, March 8-10, 2000.

9. A. Rahmel, in Molten Salt Technology, D. G. Lovering, Editor, Plenum Press, New York (1982), p. 265 ff.

10. Phase Diagrams for Ceramists – Vol. VII, L. P. Cook and H. F. McMordie, Editors, American Ceramic Society, Westerville, OH, (1989), p. 36.

11. D. C. Smith, J. M. Chavez, E. E. Rush and C. W. Matthews, "Report of the Test of the Molten-Salt Pump and Valve Loops", Sandia National Laboratories, SAND91-1747, February 1992.

12. B. W. Hatt, in Molten Salt Technology, D. G. Lovering, Editor, p. 395 ff, Plenum Press, New York, 1982.

13. D. A. Nissen and D. E. Meeker, Inorg. Chem., 22, 716 (1983).

14. D. H. Kerridge, “Chemistry of Molten Nitrates and Nitrites”, in MTP International Review of Science, C. C. Addison and D. B. Sowerby, Editors, Vol. 2, p. 29 (1972).

15. R. W. Mar and C. M. Kramer, Solar Energy Mater., 5, 71 (1981).

16. A. S. Nagelberg and R. W. Mar, "Thermochemistry of Nitrate Salts", Sandia National Laboratories, SAND81-8879, January 1982.
17. W. H. Smyrl, "Corrosion in Molten Salts Used for Solar Thermal Storage Applications", Sandia National Laboratories, SAND78-0246C, Dec. 1978.

18. G. J. Janz, C. B. Allen, N. P. Bansal, R. M. Murphy and R. P. T. Tomkins, "Physical Properties Data Compilations Relevant to Energy Storage. Vol. II. Molten Salts", National Bureau of Standards, NSRDS-NBS 61, Part II, April 1979.

19. R. W. Bradshaw and R. W. Carling, Proceedings, Joint International Symposium on Molten Salts, The Electrochemical Society, Vol. 87-7, p. 959, Sept. 1987.

20. E. G. Bohlmann, “Heat Transfer Salt for High Temperature Steam Generation”, Oak Ridge National Laboratory, ORNL-TM-377-7, Dec. 1972.

21. S. H. Goods, R. W. Bradshaw, M. R. Prairie and J. M. Chavez, “Corrosion of Stainless and Carbon Steels in Molten Mixtures of Industrial Nitrates”, Sandia National Laboratories, SAND94-8211, March 1994.

22. R. W. Bradshaw, S. H. Goods, M. R. Prairie and D. R. Boehme, Proceedings, International Symposium on Molten Salt Chemistry and Technology-1993, The Electrochemical Society, PV-93-9, p. 446, May 1993.

23. R. W. Bradshaw and S. H. Goods, “Corrosion of Stainless Steels during Thermal Cycling in Molten Nitrate Salts”, The Electrochemical Society, 191st Meeting, Montreal, Canada, May 8, 1997.

24. R. W. Bradshaw, Corrosion (N.A.C.E.), 43 (3) (1987), p. 173.

25. R. W. Bradshaw, "Corrosion of 304SS by Molten $NaNO_3$-KNO_3 in a Thermal Convection Loop", Sandia National Laboratories, SAND80-8856, December 1980.

26. Martin-Marietta Corp., "Advanced Central Receiver Power System, Phase II, Vol. III. Molten Salt Materials Tests", Sandia National Laboratories, Contractor report SAND81-8192/3, Jan. 1984.

27. J. Armitt, D. R. Holmes, M. I. Manning, D. B. Meadowcroft and E. Metcalf, "The Spalling of Steam Grown Oxide from Superheater and Reheater Tube Steels”, Central Electricity Generating Board (U.K.), RD/L/R-1974, February 1978.

28. J. J. Stephens, R. E. Semarge and R. W. Bradshaw, in Microbeam Analysis-1986, A. D. Romig and W. F. Chambers, Editors, Microbeam Analysis Society, (1986), p. 337.

29. P. Hancock, Mater. Sci. Tech., 3 (1987), p. 536.

30. W. S. Winters, R. W. Bradshaw and F. W. Hart, "Design and Operation of Thermal Convection Loops for Corrosion Testing in Molten $NaNO_3$-KNO_3", Sandia National Laboratories, SAND80-8212, June 1980.

31. P. F. Tortorelli and J. H. DeVan, "Thermal Convection Loop Study of the Corrosion of Fe-Ni-Cr Alloys by Molten $NaNO_3$-KNO_3", Oak Ridge National Laboratory, ORNL TM-8298, Dec. 1982.

32. J. W. Slusser, J. B. Titcomb, M. T. Heffelfinger, and B. R. Dunbobbin, J. Metals, 37 (7) (1985), p. 24.

33. D. R. Boehme and R. W. Bradshaw, High Temp. Sci., 18 (1984), p. 39.

34. R. W. Bradshaw, "Thermal Convection Loop Corrosion Tests of 316SS and IN800 in Molten Nitrate Salts", Sandia National Laboratories, SAND82-8210, Feb. 1982.

35. R. W. Bradshaw, "Oxidation and Chromium Depletion of Alloy 800 and 316SS in Molten $NaNO_3$-KNO_3 at Temperatures above 600°C", Sandia National Laboratories, SAND86-9009, Jan. 1987.

36. R. W. Bradshaw and S. H. Goods, “Effect of Temperature on Corrosion of Type 316SS in Molten Nitrate Salts”, The Electrochemical Society, 197th Meeting, Toronto, Canada, May 12, 2000.

37. P. Spiteri, "Corrosion of Different Steels in Na-K-Nitrate-Nitrite Mixtures (HTS)", Molten Nitrate Salt Workshop, Sandia National Laboratories, October 29-30,1980.

38. W. E. Kirst, W. M. Nagle and J. B. Castner, Trans A. I. Ch. E., 36 (1941), p. 361.

39. Y. I. Sorokin and K. L. Tseitlin, Khim. Prom., 41 (1965), p. 64.

40. C. M. Kramer, W. H. Smyrl and W. B. Estill, J. Mater. Energy Sys., 1 (4), (1980), p. 59.

41. R. W. Bradshaw, “Oxidation of Cr-Mo Steels in Molten Sodium-Potassium Nitrate”, TMS-AIME, Fall Meeting, Philadelphia, PA, Oct. 3, 1982.

42. M. R. Taylor, J. M. Calvert, D. G. Lees, and D. B. Meadowcroft, Oxid. Met., 14 (1980), p. 499.

43. S. H. Goods, R. W. Bradshaw, M. J. Clift and D. R. Boehme, “The Effect of Silicon on the Corrosion Characteristics of $2^1/_4$Cr -1Mo Steel in Molten Nitrate Salt”, SAND 97-8269, October 1997.

44. A. Baraka, A. I. Abdel-Rohman and A. A. El Hosary, Brit. Corros. J., 11(1) (1976), p. 44.

45. T. Ishikawa and T. Sasaki, Proc. Eighth Int'l. Congress on Metallic Corrosion (1981), p. 803.

46. I. B. Singh and U. Sen, Brit. Corros. J., 27(4) (1992), p. 299.

47. R. W. Bradshaw, S. H. Goods and M. J. Clift, Sandia National Laboratories, unpublished data.

48. W. Z. Friend, Corrosion of Nickel and Nickel-Base Alloys, Wiley-Interscience (1980), p. 191.

49. V. P. Burolla and J. J. Bartel, "High Temperature Compatibility of Nitrate Salts, Granite Rock and Pelletized Iron Ore", Sandia National Laboratories, SAND79-8634, Aug. 1979.

50. R. W. Bradshaw, Sandia National Laboratories, in preparation.

51. R. H. Bricknell and D. A. Woodford, Acta Met., 30 (1982), p. 257.

52. S. H. Goods, J. Mater. Energy Sys., 5 (1983), p. 28.

53. S. H. Goods, in High Temperature Corrosion in Energy Systems, M. F. Rothman, Editor, The Metallurgical Society, Warrendale, PA (1985), p. 643.

54. J. L. Kaae, "Final Report on Low-Cycle Fatigue and Creep-Fatigue Testing of Salt-Filled Alloy 800 Specimens", General Atomic Co., Sandia Contractor report, SAND 82-8182, May 1982.

55. S. H. Goods, Metall. Trans. A, 14A (1985), p. 1031.

X. DISTRIBUTION

1 Advanced Thermal Systems, Inc.
Attn: Mr. Robert Thomas
5031 W. Red Rock Drive
Larkspur, CO 80118-9053

1 Boeing Company
Attn: Mr. Bob Litwin
6633 Canoga Avenue
PO Box 7922 - Mail Code LA38
Canoga Park, CA 91309-7922

1 Boeing Company
Attn: Michael W. McDowell
6633 Canoga Ave. MC T038
P.O. Box 7922
Canoga Park, CA 91309-7922

1 Boeing Company
Attn: Dale Rogers
6633 Canoga Avenue
PO Box 7922 - Mail Code LA38
Canoga Park, CA 91309-7922

1 CIEMAT – Madrid
Attn: Manuel Romero Alvarez
Institudo de Energias Renovables
Avda. Complutense, 22
E-28040 Madrid
SPAIN

1 CIEMAT-PSA
Attn: Manuel J.Blanco Muriel
Apartado 22
E-04200 Tabernas (Almeria)
SPAIN

1 Edison International Corp.
Attn: Mr. Paul Lee
7103 Marcelle Street
Paramount, CA 90723

1 Ignacio Grimaldi Pastoril
Ghersa
Avda. del Puerto N 1-6
11006 Cadiz
SPAIN

1 Jose Benevente Sierra
Avda. del Puerto N 1-6
11006 Cadiz
SPAIN

1 Kearney & Associates
Attn: Mr. David W. Kearney
PO Box 2568
Vashon, WA 98070

1 KJC Operating Company
Attn: Scott D. Frier
41100 Highway 395
Boron, CA 93516-2109

1 Nagle Pumps, Inc.
Attn: Daniel L. Barth
1249 Center Avenue
Chicago Heights, IL 60411

1 Nagle Pumps, Inc.
Attn: James Nagle
1249 Center Avenue
Chicago Heights, IL 60411

1 Nexant, Inc.
Attn: Mr. William R. Gould, Jr.
45 Fremont St., 7th Floor
San Francisco, CA 94105-2210

1 Nexant, Inc.
Attn: Mr. Bruce Kelly
45 Fremont St., 7th Floor
San Francisco, CA 94105-2210

1 Nexant, Inc.
Attn: Mr. Alex Zavocio
45 Fremont St., 7th Floor
San Francisco, CA 94105-1895

1 PacifiCorp
Attn: Mr. Ian Andrews
Utah Power Generation Engineering
1407 West North Temple
Salt Lake City, UT 84140-0001

1 Pitt-Des Moines, Inc.
Attn: John C. Dewey
9719 Lincoln Village Drive, Suite 301
Sacramento, CA 95827

1 Salt River Project

Attn: Mr. Ernie Palomino
P. O. Box 52025
Mail Station ISB664
Phoenix, AZ 85072-2025

1 Tom Tracey
6922 S. Adams Way
Littleton, CO 80122

1 U. S. Department of Energy EE-11
Attn: Tommy Rueckert
1000 Independence Avenue SW
Washington, DC 20585

1 U. S. Department of Energy EE-11
Attn: Glenn Strahs
1000 Independence Avenue, SW
Washington, DC 20585

1 U. S. Department of Energy EE-11
Attn: Mr. Frank (Tex) Wilkins
1000 Independence Avenue, SW
Washington, DC 20585

1 University of Houston
Attn: Dr. Lorin Vant-Hull
Physics Department 5506
4800 Calhoun Road
Houston, TX 77204-5506

1 MS 0703 James Pacheco, 6216
1 MS 0703 Craig Tyner, 6216
1 MS 0703 Hugh Reilly, 6216
1 MS 0752 Earl Rush, 6218
1 MS 1127 Solar Tower Library

1 MS 9001 M. E. John, 8000
Attn: R. C. Wayne, 2800, MS 9005
J. Vitko, 8100, MS 9004
W. J. McLean, 8300, MS 9054
D. R. Henson, 8400, MS 9007
P. N. Smith, 8500, MS 9002
K. E. Washington, 8900, MS 9003
1 MS 9042 D. B. Dawson, 8725
5 MS 9402 R. W. Bradshaw, 8722
5 MS 9404 S. H. Goods, 8725
1 MS 9405 R. H. Stulen, 8700
Attn: J. M. Hruby, 8702, MS 9401
W. Bauer, 8704, MS 9161
R Q. Hwang, 8721, MS 9161
W. R. Even, 8722, MS 9403
J. C. F. Wang, 8723, MS 9403
K. L. Wilson, 8724, MS 9402
J. Garcia, 8725, MS 9401

E. P. Chen, 8726, MS 9161
J. L. Handrock, 8727, MS 9042
M. F. Horstemeyer, 8728, MS 9042
C. C. Henderson, 8729, MS 9401
J. E. M. Goldsmith, 8730, MS 9409
W. C. Replogle, 8731, MS 9409
G. D. Kubiak, 8732, MS 9409

3	MS 9018	Central Technical Files, 8945-1
1	MS 0899	Technical Library, 9616
1	MS 9021	Classification Office, 8511/Technical Library, MS 0899, 9616
1	MS 9021	Classification Office, 8511 for DOE/OSTI